Available online at www.sciencedirect.com
ScienceDirect
ELSEVIER
Journal of the European Ceramic Society 29 (2009) 2363–2367
ECERS
www.elsevier.com/locate/jeurceramsoc

Wetting and adhesion of Si on Si_3N_4 and BN substrates

B. Drevet[a,*], R. Voytovych[b], R. Israel[a,b], N. Eustathopoulos[b]

[a] *CEA INES-RDI, LITEN/DTS/LCS, BP 322 Savoie Technolac, 50 av. du Lac Léman, 73377 le Bourget du Lac, France*
[b] *SIMAP – ENSEEG, INPG, Domaine Universitaire, BP 75, 1130 rue de la Piscine, 38402 Saint-Martin d'Hères Cedex, France*

Received 13 October 2008; received in revised form 23 December 2008; accepted 8 January 2009
Available online 27 February 2009

Abstract

Wetting, adhesion and reactivity are the principal factors determining the capability of a solid to be used as mould material. In this work wetting of silicon and boron nitrides by molten silicon is studied in neutral gas atmosphere by the sessile drop technique at temperatures close to the silicon melting point. Adhesion is qualified by the behaviour of solidified droplets under the effect of thermo-mechanical stresses generated during cooling at room temperature. The reactivity at silicon/nitride interfaces is studied by scanning electron microscopy and EDX-microanalysis.
© 2009 Elsevier Ltd. All rights reserved.

Keywords: Interfaces; Nitrides

1. Introduction

Currently photovoltaic silicon is produced mainly by liquid route techniques such as ingot growth and ribbon technologies. They involve the use of foreign materials in contact with molten silicon, i.e. crucibles or substrates. The two main requirements for crucible materials are (i) negligible reactivity to avoid pollution of the silicon and to increase the lifetime of the crucible, and (ii) non-wetting behaviour (i.e. contact angles θ much higher than 90°) which is a favourable condition for obtaining a spontaneous detachment of solidified silicon from the crucible walls under the effect of thermo-mechanical stresses.[1,2] In specific cases, for instance when processing silicon ribbons by solidification on a foreign substrate passing through a liquid bath, good wetting ($\theta \ll 90°$) is required for the substrate material.[3] In this case dense materials must be employed in order to avoid infiltration of open porosities by silicon.

In this work, wetting, reactivity and adhesion of silicon and boron nitrides by molten silicon are studied at temperatures close to its melting point. Silicon nitride is of considerable interest because the growth of photovoltaic silicon ingots is currently performed in crucibles coated with a silicon nitride powder which acts as an interface releasing agent between silicon and the crucible.[4] Moreover, literature values of contact angle in the Si/Si_3N_4 system have a very wide spread, ranging from 0° to 90°[1,5–8] (Table 1). Adhesion occurs between Si and Si_3N_4 (Table 1), which seems contradictory with the use of this ceramic as a releasing agent. As for boron nitride, its main drawback is boron contamination which leads to overdoping of silicon. Nevertheless, BN is of great interest, for instance as crucible material for studying physicochemical and physical properties of molten Si and Si alloys, as it is one of the very few materials (and probably the only one) that are non-wetted by liquid silicon ($\theta > 90°$). However, literature data of contact angles indicate a wide range of values, lying between 95° and 145°, and contradictory results are obtained for adhesion[1,5,8,9] (Table 2). These literature data justify the work carried out here.

2. Experimental procedure

Si_3N_4 samples were processed by sintering using Y_2O_3 and Al_2O_3 (both 6 wt.%) as sintering aids. The residual porosity is less than 2%. The samples were mechanically polished using diamond paste up to an average roughness $R_a = 70$ nm. The purity of pyrolytic BN used in this study was higher than 99%. The average roughness R_a of the substrate surface after polishing with diamond paste up to 1 μm was about 30 nm. For comparison purposes a point experiment was performed on vitreous silica with an average surface roughness of a few nm. Electronic grade silicon was used to form the liquid phase.

* Corresponding author. Tel.: +33 4 79 44 45 95; fax: +33 4 79 62 37 71.
E-mail address: beatrice.drevet@cea.fr (B. Drevet).

0955-2219/$ – see front matter © 2009 Elsevier Ltd. All rights reserved.
doi:10.1016/j.jeurceramsoc.2009.01.024

Table 1
Literature data for the Si/Si_3N_4 system.

Si_3N_4	Atmosphere	Temperature (°C)	Time	θ (°)	Adhesion	Reference
Sintered, 99.5 wt.% (0.22 wt.% Al)	Ar ($P(O_2) \approx 10^{-15}$ Pa)	1420	1200 s	89	–	[5]
Sintered (3% Al_2O_3, 2% La_2O_3, 1% Y_2O_3)	Gettered Ar (Zr) Gettered Ar (Ta)	1450	Several hours	0[a] 48[a]	–	[6]
CVD	Buffer gas ($P(O_2) \approx 10^{-15}$ Pa)	1430	3600 s	48–52	–	[7]
Hot-pressed, no binder	Inert gas	1412	300 s	51	Yes	[1]
Polycrystalline	Vacuum	1500	–	<40	Yes	[8]

[a] Measured at room temperature

Wetting was studied by the sessile drop method in a metallic chamber furnace. The device is induction heated by coupling on a graphite susceptor. The working zone is surrounded by a graphite thermal insulator. A vacuum unit allows a total pressure of 10^{-4} Pa to be attained at ambient temperature. The presence of graphite inside the furnace allows atmospheres with a very low oxygen partial pressure $P(O_2)$ to be obtained. Experiments were carried out in an Ar flow. A sessile drop experiment consists in placing a 50–100 mg piece of silicon on a solid substrate inside the furnace at room temperature. Heating is performed under vacuum up to 600 °C, then Ar is introduced and the temperature is increased up to the holding temperature of 1430 °C. The furnace is equipped with windows enabling the melting and spreading processes to be filmed with a video camera (25 frames/s). The camera is connected to a computer for automatic image analysis. The drop base radius R and contact angle θ are extracted with an accuracy of ±2% and ±3°, respectively.

In order to check the effect of furnace atmosphere on wettability results, few experiments were performed in another furnace consisting of an alumina chamber heated with a resistance and connected to a high vacuum pump system. The atmosphere is a static neutral gas previously purified by passing it through a bed of Zr–Al getter heated to 400 °C. In this gas, $P(O_2)$ is lower than 10^{-13} Pa.[10] The results obtained in the two furnaces do not differ significantly. After cooling, selected specimens were cut perpendicular to the interface, embedded in resin and polished for optical and SEM characterisation.

3. Results and discussion

3.1. Si_3N_4

Fig. 1 shows the wetting curves (contact angle and drop base diameter) for molten Si on Si_3N_4. The time $t = 0$ corresponds to complete melting of Si. The initial contact angle, equal to $\theta_0 = 82 \pm 3°$, decreases rapidly to a final value $\theta_F = 49 \pm 3°$ in about 200 s. After cooling to room temperature, the solidified drop apparently adheres to the substrate. However, cracking occurred partly along the interface and partly inside the Si drop (Fig. 2). As expected for the non-reactive Si/Si_3N_4 system, no reaction product visible at the SEM scale (about 0.2 μm) is formed at the interface.

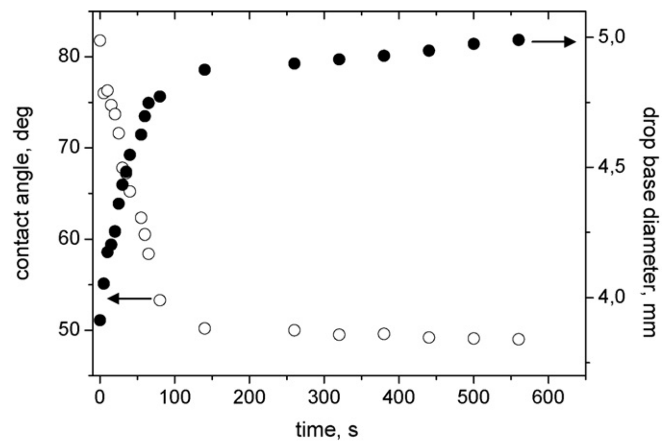

Fig. 1. Contact angle and drop base diameter as a function of time for a Si drop on sintered Si_3N_4 at 1430 °C.

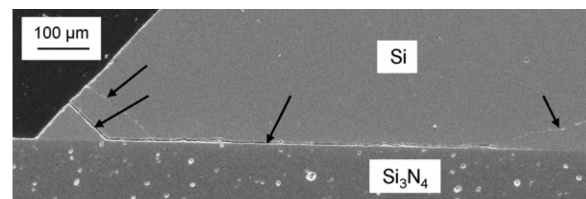

Fig. 2. Cross-section of a Si/Si_3N_4 sample (SEM). The arrows indicate cracks.

Table 2
Literature data for the Si/BN system.

BN	Atmosphere	Temperature (°C)	Time	θ (°)	Adhesion	Reference
Pyrolytic BN (99.6 wt.%)	Ar ($P(O_2) \approx 10^{-15}$ Pa)	1420	1200 s	144	–	[5]
Hot-pressed, no binder	Inert gas	1412	300 s	122	No	[1]
Cubic Hexagonal	Vacuum	1500	–	95 110	–	[9]
Pyrolytic BN	Vacuum	1500	–	105	Yes	[8]

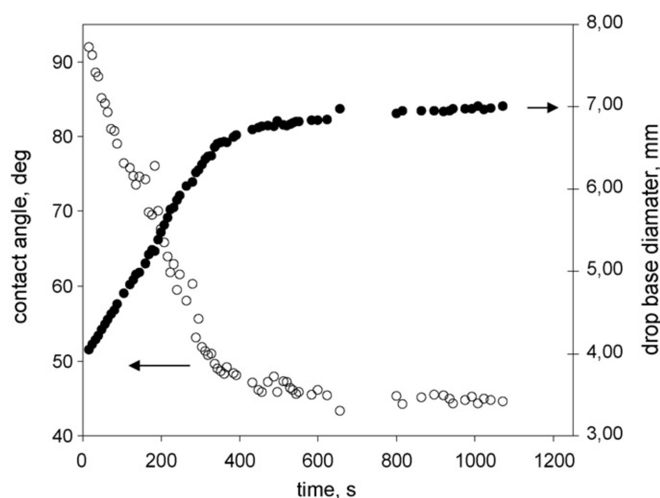

Fig. 3. Contact angle and drop base diameter as a function of time for a Si drop on pre-oxidised sintered Si_3N_4 at 1430 °C.

For non-reactive metal/solid (ceramic or metallic) systems, the spreading time for millimetric sized droplets is of the order of 10^{-2} s.[11–13] This time is four orders of magnitude lower than the spreading time observed in the Si/Si_3N_4 system. Such long spreading times are observed in reactive metal/ceramic systems when the reaction at the solid/liquid/vapour triple line controls the spreading rate.[14,15] In the Si/Si_3N_4 system, the long spreading rate is attributed to the deoxidation of the Si_3N_4 surface by reaction between molten Si and the SiO_2 skin on Si_3N_4. Indeed, it has long been established that a fresh Si_3N_4 surface in contact with air at room temperature is covered instantaneously by a nanometric oxide skin with a thickness of about 0.5 nm.[16] In our experimental conditions, this film persists up to the experimental temperature of 1430 °C, as testified by the value of the initial contact angle $\theta_0 = 82 \pm 3°$. Indeed, an experiment performed with a silica substrate led to an equilibrium contact angle obtained instantaneously after Si melting (i.e. without measurable kinetics) of $83 \pm 4°$, very close to the initial contact angle measured on Si_3N_4. Further evidence is given by another sessile drop experiment performed on Si_3N_4 pre-oxidised at 900 °C in air for 2 h. Under these conditions, it is expected that Si_3N_4 is covered by an SiO_2 layer with a thickness of several nm.[16] With this substrate, the initial contact angle is $\theta_0 = 92 \pm 3°$ (Fig. 3), close to the angle on bulk SiO_2. Clearly, the initial contact angles in the experiments given in Figs. 1 and 3 are on SiO_2 and not on Si_3N_4. However, immediately after melting, the contact angle starts to decrease, first rapidly and then more slowly, and tends towards its equilibrium value. This is attributed to deoxidation of Si_3N_4 by reaction between molten Si and the oxide skin at the solid–liquid–vapour triple line, according to equation:

$$\langle SiO_2\rangle + (Si) \rightarrow 2[SiO] \quad (1)$$

where the symbols ⟨⟩, () and [] denote solid, liquid and gas phases, respectively. The detailed mechanism of this three-phase reaction was discussed and modelled in a similar system consisting of a Si alloy on oxidised SiC.[14] It was concluded in particular that (i) the drop base diameter increases with time linearly and

Table 3
Contact angles of Si on oxide substrates at a temperature close to Si melting point.

Oxide	Contact angle θ (°)	
	Ref.[5]	Ref.[1]
SiO_2	85	96
Al_2O_3	86	93
MgO	88	82
Ta_2O_5	–	85
ZrO_2	–	80

(ii) for oxide skin thicknesses less than 100 nm, deoxidation kinetics becomes virtually independent of skin thickness. Both these conclusions are also valid for the Si/Si_3N_4 system (see Figs. 1 and 3).

According to the previous discussion, the equilibrium contact angle of Si on deoxidised sintered Si_3N_4 is $\theta_F = 49 \pm 3°$. However, as specified in Section 2, the Si_3N_4 used in the present work contains several % of Al and Y oxides. These oxides can affect the contact angle of Si_3N_4, as predicted by Cassie's equation[17]:

$$\cos\theta_C = \alpha_{ox}\cos\theta_{ox} + (1 - \alpha_{ox})\cos\theta_{Si_3N_4} \quad (2)$$

where the subscript C refers to Cassie while α_{ox} is the volume fraction of oxides. In the literature it is well established that the contact angle of Si on stable oxides is around 90°. This is true not only for silica substrates (see previous paragraph) but also for Al_2O_3, MgO, ZrO_2 or Ta_2O_5 (Table 3). Application of Eq. (2) taking $\theta_C = 49°$, $\theta_{ox} = 90°$ and $\alpha_{ox} = 0.1$ leads to a value $\theta_{Si_3N_4} = 43 \pm 3°$ for the intrinsic contact angle of Si on Si_3N_4.

The equilibrium contact angle obtained in this study is in acceptable agreement with the angles measured by Barsoum and Ownby[7] and by Maeda et al.[1] considering the different types of Si_3N_4 used by the authors (Table 1). In order to decrease $P(O_2)$, Li and Hausner[6] performed their experiments in closed crucibles made of Zr or Ta, i.e. metals featuring a strong affinity for oxygen. The samples were maintained at the silicon melting temperature for several hours and contact angles were measured after cooling on the solidified drops. According to these authors, the value of 48° is the contact angle on an oxidised surface of Si_3N_4 substrate whereas the value of 0° is the true contact angle on Si_3N_4 (see Table 1). Our results are not in agreement with the interpretation of Li and Hausner since we show above that the contact angle on oxidised Si_3N_4 is 82–92°. The value of 0° obtained by these authors is probably due to decomposition of Si_3N_4. Indeed, according to the values of standard Gibbs energy of formation (/nitrogen gram atom) at 1430 °C, ZrN is much more stable than Si_3N_4 (−203 kJ against −46 kJ[18]) so that the following reactions become thermodynamically favourable:

$$\text{on the substrate surface: } \langle Si_3N_4\rangle \rightarrow 3(Si) + 2[N_2] \quad (3)$$

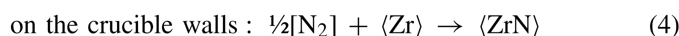

$$\text{on the crucible walls: } \tfrac{1}{2}[N_2] + \langle Zr\rangle \rightarrow \langle ZrN\rangle \quad (4)$$

Confirmation of this result could have been obtained by analysing the free surface of the substrate or the surface of the metallic crucible after the experiment. However, such analyses were not done by the authors. Note the good agreement between

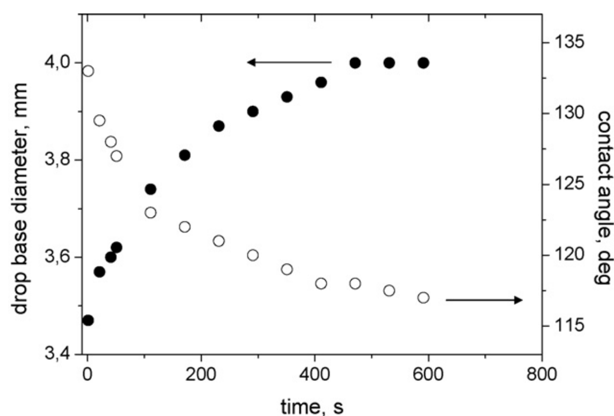

Fig. 4. Contact angle and drop base diameter as a function of time for a Si drop on pyrolytic BN at 1430 °C.

our results and the value of 48° measured by Li and Hausner when a Ta crucible was used. This indicates that decomposition of Si_3N_4 according to reaction (3) should not occur in this case, and this is consistent with the fact that the thermodynamic stability of TaN is less than that of ZrN (at 1430 °C the standard Gibbs energy of formation of TaN is −128 kJ/mol against −203 kJ/mol for ZrN[18]). In view of our results concerning the initial contact angle, it can be concluded that the value of 89° found by Yuan et al.[5] (Table 1) was measured on an oxidised substrate.

In the growth of photovoltaic silicon, usually performed in inert gas or in vacuum, it is well-known that the solidified ingot can pull off the mould without adhesion when the mould walls are coated with a layer of Si_3N_4 powder. This is in contradiction with literature results and those obtained in this work showing that Si_3N_4 is well-wetted by liquid Si and that cracks produced during cooling under the effect of thermo-mechanical stresses occur partly in the Si bulk (Fig. 2). More work (now in progress) is needed in order to understand the specific chemistry of heat-treated Si_3N_4 powder applied to crucible surfaces and its effect on wetting and adhesion.

3.2. BN

As shown by Fig. 4 the contact angle on BN decreases from an initial value $\theta_0 = 133 \pm 3°$ to a steady contact angle $\theta_F = 117 \pm 3°$ in about 10 min. Neither the contact angle nor the drop base diameter d changed measurably even after 60 min of holding at 1430 °C. As in the Si/Si_3N_4 system, spreading kinetics can be assumed to be controlled by deoxidation of BN, which is in fact also an oxidisable material. However, this hypothesis does not match with the two following considerations. (i) Boron oxide (B_2O_3) is volatile. As a result, even at temperatures close to 1000 °C (at this temperature $P_{B_2O_3} = 10^{-2}$ Pa[18]) rapid cleaning of the BN surface should take place in low $P(O_2)$ environments.[11] (ii) As shown by the results of Table 3 the contact angle of Si on oxides is around 90°, i.e. much lower than the initial contact angle of 133° observed on BN (Fig. 4). From this discussion it is very unlikely that the $\theta(t)$ and $d(t)$ curves of Fig. 4 result from BN deoxidation.

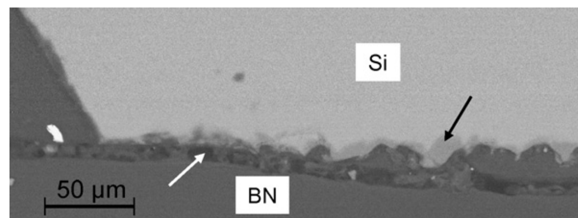

Fig. 5. Si/BN interface close to the triple line (SEM). The black arrow indicates the Si_3N_4 reaction layer and the white arrow the crack.

An alternative explanation is to assume that the initial contact angle of 133° is the contact angle of Si on the unreacted BN and that the observed spreading kinetics results from interface modification due to the reaction between Si and BN forming Si_3N_4:

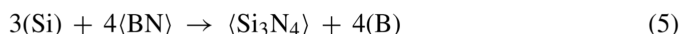

$$3(\mathrm{Si}) + 4\langle \mathrm{BN} \rangle \rightarrow \langle \mathrm{Si_3N_4} \rangle + 4(\mathrm{B}) \quad (5)$$

The thermodynamic stability of BN is higher than that of Si_3N_4 (the standard Gibbs energy of formation of Si_3N_4/nitrogen gram atom at 1430 °C is −46 kJ against −101 kJ for BN[18]). However, some limited reaction can occur driven by the partial Gibbs energy of mixing of boron in molten silicon. Such a reaction was indeed observed at the Si/BN interface leading to the formation of a layer with an average thickness e of about 10 µm (Fig. 5). EDX chemical analysis shows the presence of only silicon and nitrogen in the layer. The thickness of this layer varies from place to place and in some cases the layer was not thick enough to be observed by standard SEM. An experiment performed at the same temperature by increasing the holding time from 10 to 60 min did not lead to a measurable increase in the average layer thickness.

As Si_3N_4 is wetted much better by Si than BN, the formation of Si_3N_4 at the interface must improve wetting. If so, spreading kinetics in the Si/BN system would be controlled by the rate of growth of the reaction product (in this case Si_3N_4) parallel to the interface at the substrate/liquid/vapour line as proposed in the model of reactive wetting described in Refs.[11,19] However, according to this model, the final contact angle in a reactive system is equal to the contact angle on the reaction product. This does not agree with the results of our experiments showing that the final contact angle on BN is 117°, much higher than the contact angle of 49° observed with Si_3N_4.

A possible explanation of this (apparent) disagreement between model prediction and experimental findings is that the liquid Si reacting with the substrate is saturated in B before the drop attains the contact angle of Si/Si_3N_4 system. This hypothesis can be checked by assuming that the drop attains the contact angle $\theta \approx 49°$ by forming a Si_3N_4 reaction layer 10 µm thick and then calculating the corresponding mole fraction x_B of boron released into the drop.

This calculation is performed for the droplet of the experiment presented in Fig. 4. This droplet has a volume of 36 mm^3 and contains 3.1×10^{-3} mol of Si. Assuming a spherical cap shape and taking $\theta = 49°$, the base drop diameter d is found to be 7.22 mm. The number of Si_3N_4 moles contained in a layer with base diameter $d = 7.22$ mm and thickness $e = 10$ µm is

1.0×10^{-5}, and thus, according to reaction (5), the number of B moles released into the Si is 4.0×10^{-5}. This value corresponds to a mole fraction of dissolved B $x_B = 1.3 \times 10^{-2}$ which is one order of magnitude higher than the equilibrium value 1.4×10^{-3} found by Yuan et al.[5] for molten silicon equilibrated with BN at 1420 °C. This calculation confirms the hypothesis that chemical equilibrium is established well before the equilibrium contact angle on the reaction product layer is attained.

The steady contact angle of 117° observed on BN is much lower than the contact angle obtained by Yuan et al.[5] The agreement with the results of Maeda et al.[1] and of Naidich for hexagonal BN[9] (Table 2) can be considered as acceptable taking into account the numerous factors affecting wetting (roughness of substrate surface, type and concentration of impurities in the solid and liquid phases, partial pressure of oxygen[20]).

After cooling to room temperature, the solidified drop seems to adhere to the substrate. However, as shown in Fig. 5, extensive cracking is observed. Crack propagation occurs mainly inside bulk BN, close to and parallel to the interface. In some cases this cracking is so extensive that the solidified drop can be removed easily from the substrate. The type of rupture observed in Si/BN samples (cohesive rupture in bulk BN) is very different from the rupture observed for Si/Si_3N_4 samples (Fig. 2). This difference can be explained by the weak energy of cohesion between hexagonal planes of pyrolytic BN, leading to a low energy of cohesive rupture.

4. Conclusions

The steady contact angles observed for millimetre sized droplets of silicon on sintered silicon nitride and pyrolytic boron nitride are equal to $49 \pm 3°$ and $117 \pm 3°$, respectively. For both nitrides spreading kinetics are typical of reactive wetting. On silicon nitride the spreading rate is controlled by deoxidation of the substrate by reaction between silicon and the oxide film with formation of the volatile silicon monoxide. On boron nitride the spreading kinetics is limited by the rate of formation of silicon nitride at the interface, by reaction between silicon and boron nitride. However, the reactivity in the Si/BN system is so weak that chemical equilibrium (saturation of B in liquid Si) is established well before the equilibrium contact angle on the reaction product (i.e. Si_3N_4) is attained. In both Si/Si_3N_4 and Si/BN systems apparent adhesion is observed at room temperature. However, in both cases extensive cracking occurs under the effect of thermo-mechanical stresses. The cracking path is different in the two systems, mixed (partly interfacial and partly in bulk Si) in the case of Si/Si_3N_4 and cohesive, in bulk BN, in the case of Si/BN.

Acknowledgements

Fruitful discussions with Dr. J.P. Garandet and Dr. D. Camel are gratefully acknowledged.

References

1. Maeda, Y., Yokoyama, T., Hide, I., Matsuyama, T. and Sawaya, K., Releasing material for the growth of shaped silicon crystals. *J. Electrochem. Soc.*, 1986, **133**, 440–443.
2. Cröll, A., Lantzsch, R., Kitanov, S., Salk, N., Szofran, F. R. and Tegetmeier, A., Melt-crucible wetting behavior in semiconductor melt growth systems. *Cryst. Res. Technol.*, 2003, **38**, 669–675.
3. Beck, A., Geissler, J. and Helmreich, D., Substrate development for the growth of silicon foils by ramp assisted foil casting technique (RAFT). *J. Cryst. Growth*, 1990, **104**, 113–118.
4. Saito, T., Shimura, A. and Ichikawa, S., A new directional solidification technique for polycrystalline solar grade silicon. In *XV IEEE Photovoltaic Specialists Conference*, 1981, pp. 576–580.
5. Yuan, Z., Huang, W. L. and Mukai, K., Wettability and reactivity of molten silicon with various substrates. *Appl. Phys. A*, 2004, **78**, 617–622.
6. Li, J. G. and Hausner, H., Influence of oxygen partial pressure on the wetting behaviour of silicon nitride by molten silicon. *J. Eur. Ceram. Soc.*, 1992, **9**, 101–105.
7. Barsoum, M. W. and Ownby, P. D., The effect of oxygen partial pressure on the wetting of SiC, AlN and Si_3N_4 by Si and a method for calculating the surface energies involved. In *Surfaces and Interfaces in Ceramic and Ceramic–Metal Systems*, ed. J. Pask and A. Evans. Plenum Press, New York, 1981, pp. 457–466.
8. Champion, J. A., Keene, B. J. and Allen, S., Wetting of refractory materials by molten metallides. *J. Mater. Sci.*, 1973, **8**, 423–426.
9. Naidich, Y. V., The wettability of solids by liquid metals. In *Progress in Surface and Membrane Science*, *vol. 14*, ed. D. A. Cadenhead and J. F. Danielli. Academic Press, New York, 1981, pp. 353–484.
10. Parra, R., Voytovych, R. and Eustathopoulos, N., Wetting of MgO by Cu_2S–FeS melts. *Metall. Mater. Trans. B*, 2007, **38**, 347–349.
11. Eustathopoulos, N., Nicholas, M. and Drevet, B., Wettability at high temperature. *Pergamon Materials Series*, *vol. 3*. Pergamon, Oxford, UK, 1999.
12. Saiz, E. and Tomsia, A. P., Atomic dynamics and Marangoni films during liquid–metal spreading. *Nat. Mater.*, 2004, **3**, 903–909.
13. Naidich, Y. V., Zabuga, V. V. and Perevertailo, V. M., Temperature effect on the kinetics of spreading and wetting in systems with different character of interaction of contacting phases. *Adgeziya rasplavov i paika materialov*, 1992, **27**, 23–24.
14. Dezellus, O., Hodaj, F., Rado, C., Barbier, J. N. and Eustathopoulos, N., Spreading of Cu–Si alloys on oxidized SiC in vacuum: experimental results and modelling. *Acta Mater.*, 2002, **50**, 979–991.
15. Voytovych, R., Koltsov, A., Hodaj, F. and Eustathopoulos, N., Reactive vs non-reactive wetting of ZrB_2 by azeotropic Au–Ni. *Acta Mater.*, 2007, **55**, 6316–6321.
16. Raider, S. I., Flitsch, R., Aboaf, J. A. and Pliskin, W. A., Surface oxidation of silicon nitride films. *J. Electrochem. Soc.*, 1976, **123**, 560–565.
17. Cassie, A. B. D., Contact angles. *Discuss. Faraday Soc.*, 1948, **3**, 11–16.
18. Nist-Janaf Thermochemical Tables, *J. Phys. Chem. Ref. Data*, Monograph No. 9, 4th edition, 1998.
19. Eustathopoulos, N., Progress in understanding and modeling reactive wetting of metals on ceramics. *Curr. Opin. Solid State Mater. Sci.*, 2005, **9**, 152–160.
20. Eustathopoulos, N., Sobczak, N., Passerone, A. and Nogi, K., Measurement of contact angle and work of adhesion at high temperature. *J. Mater. Sci.*, 2005, **40**, 2271–2280.